
Spectral Correlation Hub Screening of Multivariate Time Series

Hamed Firouzi, Dennis Wei and Alfred O. Hero III

Electrical Engineering and Computer Science Department, University of Michigan,
USA firouzi@umich.edu, dlwei@eecs.umich.edu, hero@eecs.umich.edu

Summary. This chapter discusses correlation analysis of stationary multivariate Gaussian time series in the spectral or Fourier domain. The goal is to identify the hub time series, i.e., those that are highly correlated with a specified number of other time series. We show that Fourier components of the time series at different frequencies are asymptotically statistically independent. This property permits independent correlation analysis at each frequency, alleviating the computational and statistical challenges of high-dimensional time series. To detect correlation hubs at each frequency, an existing correlation screening method is extended to the complex numbers to accommodate complex-valued Fourier components. We characterize the number of hub discoveries at specified correlation and degree thresholds in the regime of increasing dimension and fixed sample size. The theory specifies appropriate thresholds to apply to sample correlation matrices to detect hubs and also allows statistical significance to be attributed to hub discoveries. Numerical results illustrate the accuracy of the theory and the usefulness of the proposed spectral framework.

Key words: Complex-valued correlation screening, Spectral correlation analysis, Gaussian stationary processes, Hub screening, Correlation graph, Correlation network, Spatio-temporal analysis of multivariate time series, High dimensional data analysis

1 Introduction

Correlation analysis of multivariate time series is important in many applications such as wireless sensor networks, computer networks, neuroimaging, and finance [1, 2, 3, 4, 5]. This chapter focuses on the problem of detecting *hub* time series, ones that have a high degree of interaction with other time series as measured by correlation or partial correlation. Detection of hubs can lead to reduced computational and/or sampling costs. For example in wireless sensor networks, the identification of hub nodes can be useful for reducing power usage and adding or removing sensors from the network [6, 7]. Hub detection can also give new insights about underlying structure in the dataset.

In neuroimaging for instance, studies have consistently shown the existence of highly connected hubs in brain graphs (connectomes) [8]. In finance, a hub might indicate a vulnerable financial instrument or a sector whose collapse could have a major effect on the market [9].

Correlation analysis becomes challenging for multivariate time series when the dimension p of the time series, i.e. the number of scalar time series, and the number of time samples N are large [4]. A naive approach is to treat the time series as a set of independent samples of a p -dimensional random vector and estimate the associated covariance or correlation matrix, but this approach completely ignores temporal correlations as it only considers dependences at the same time instant and not between different time instants. The work in [10] accounts for temporal correlations by quantifying their effect on convergence rates in covariance and precision matrix estimation; however, only correlations at the same time instant are estimated. A more general approach is to consider all correlations between any two time instants of any two series within a window of $n \leq N$ consecutive samples, where the previous case corresponds to $n = 1$. However, in general this would entail the estimation of an $np \times np$ correlation matrix from a reduced sample of size $m = N/n$, which can be computationally costly as well as statistically problematic.

In this chapter, we propose *spectral* correlation analysis as a method of overcoming the issues discussed above. As before, the time series are divided into m temporal segments of n consecutive samples, but instead of estimating temporal correlations directly, the method performs analysis on the Discrete Fourier Transforms (DFT) of the time series. We prove in Theorem 1 that for stationary, jointly Gaussian time series under the mild condition of absolute summability of the auto- and cross-correlation functions, different Fourier components (frequencies) become asymptotically independent of each other as the DFT length n increases. This property of stationary Gaussian processes allows us to focus on the $p \times p$ correlations at each frequency separately without having to consider correlations between different frequencies. Moreover, spectral analysis isolates correlations at specific frequencies or timescales, potentially leading to greater insight. To make aggregate inferences based on all frequencies, straightforward procedures for multiple inference can be used as described in Section 4.

The spectral approach reduces the detection of hub time series to the independent detection of hubs at each frequency. However, in exchange for achieving spectral resolution, the sample size is reduced by the factor n , from N to $m = N/n$. To confidently detect hubs in this high-dimensional, low-sample regime (large p , small m), as well as to accommodate complex-valued DFTs, we develop a method that we call *complex-valued (partial) correlation screening*. This is a generalization of the correlation and partial correlation screening method of [11, 9, 12] to complex-valued random variables. For each frequency, the method computes the sample (partial) correlation matrix of the DFT components of the p time series. Highly correlated variables (hubs) are then identified by thresholding the sample correlation matrix at a level

ρ and screening for rows (or columns) with a specified number δ of non-zero entries.

We characterize the behavior of complex-valued correlation screening in the high-dimensional regime of large p and fixed sample size m . Specifically, Theorem 2 and Corollary 2 give asymptotic expressions in the limit $p \rightarrow \infty$ for the mean number of hubs detected at thresholds ρ, δ and the probability of discovering at least one such hub. Bounds on the rates of convergence are also provided. These results show that the number of hub discoveries undergoes a phase transition as ρ decreases from 1, from almost no discoveries to the maximum number, p . An expression (33) for the critical threshold $\rho_{c,\delta}$ is derived to guide the selection of ρ under different settings of p , m , and δ . Furthermore, given a null hypothesis that the population correlation matrix is sufficiently sparse, the expressions in Corollary 2 become independent of the underlying probability distribution and can thus be easily evaluated. This allows the statistical significance of a hub discovery to be quantified, specifically in the form of a p -value under the null hypothesis. We note that our results on complex-valued correlation screening apply more generally than to spectral correlation analysis and thus may be of independent interest.

The remainder of the chapter is organized as follows. Section 2 presents notation and definitions for multivariate time series and establishes the asymptotic independence of spectral components. Section 3 describes complex-valued correlation screening and characterizes its properties in terms of numbers of hub discoveries and phase transitions. Section 4 discusses the application of complex-valued correlation screening to the spectra of multivariate time series. Finally, Sec. 5 illustrates the applicability of the proposed framework through simulation analysis.

1.1 Notation

A triplet $(\Omega, \mathcal{F}, \mathbb{P})$ represents a probability space with sample space Ω , σ -algebra of events \mathcal{F} , and probability measure \mathbb{P} . For an event $A \in \mathcal{F}$, $\mathbb{P}(A)$ represents the probability of A . Scalar random variables and their realizations are denoted with upper case and lower case letters, respectively. Random vectors and their realizations are denoted with bold upper case and bold lower case letters. The expectation operator is denoted as \mathbb{E} . For a random variable X , the cumulative probability distribution (cdf) of X is defined as $F_X(x) = \mathbb{P}(X \leq x)$. For an absolutely continuous cdf $F_X(\cdot)$ the probability density function (pdf) is defined as $f_X(x) = dF_X(x)/dx$. The cdf and pdf are defined similarly for random vectors. Moreover, we follow the definitions in [13] for conditional probabilities, conditional expectations and conditional densities.

For a complex number $z = a + b\sqrt{-1} \in \mathbb{C}$, $\Re(z) = a$ and $\Im(z) = b$ represent the real and imaginary parts of z , respectively. A complex-valued random variable is composed of two real-valued random variables as its real and imaginary parts. A complex-valued Gaussian variable has real and imaginary parts

that are Gaussian. A complex-valued (Gaussian) random vector is a vector whose entries are complex-valued (Gaussian) random variables. The covariance of a p -dimensional complex-valued random vector \mathbf{Y} and a q -dimensional complex-valued random vector \mathbf{Z} is a $p \times q$ matrix defined as

$$\text{cov}(\mathbf{Y}, \mathbf{Z}) = \mathbb{E} [(\mathbf{Y} - \mathbb{E}[\mathbf{Y}])(\mathbf{Z} - \mathbb{E}[\mathbf{Z}])^H],$$

where H denotes the Hermitian transpose. We write $\text{cov}(\mathbf{Y})$ for $\text{cov}(\mathbf{Y}, \mathbf{Y})$ and $\text{var}(Y) = \text{cov}(Y, Y)$ for the variance of a scalar random variable Y . The correlation coefficient between random variables Y and Z is defined as

$$\text{cor}(Y, Z) = \frac{\text{cov}(Y, Z)}{\sqrt{\text{var}(Y)\text{var}(Z)}}.$$

Matrices are also denoted by bold upper case letters. In most cases the distinction between matrices and random vectors will be clear from the context. For a matrix \mathbf{A} we represent the (i, j) th entry of \mathbf{A} by a_{ij} . Also $\mathbf{D}_{\mathbf{A}}$ represents the diagonal matrix that is obtained by zeroing out all but the diagonal entries of \mathbf{A} .

2 Spectral Representation of Multivariate Time Series

2.1 Definitions

Let $\mathbf{X}(k) = [X^{(1)}(k), X^{(2)}(k), \dots, X^{(p)}(k)]$, $k \in \mathbb{Z}$, be a multivariate time series with time index k . We assume that the time series $X^{(1)}, X^{(2)}, \dots, X^{(p)}$ are second-order stationary random processes, i.e.:

$$\mathbb{E}[X^{(i)}(k)] = \mathbb{E}[X^{(i)}(k + \Delta)] \quad (1)$$

and

$$\text{cov}[X^{(i)}(k), X^{(j)}(l)] = \text{cov}[X^{(i)}(k + \Delta), X^{(j)}(l + \Delta)] \quad (2)$$

for any integer time shift Δ .

For $1 \leq i \leq p$, let $\mathbf{X}^{(i)} = [X^{(i)}(k), \dots, X^{(i)}(k + n - 1)]$ denote any vector of n consecutive samples of time series $X^{(i)}$. The n -point Discrete Fourier Transform (DFT) of $\mathbf{X}^{(i)}$ is denoted by $\mathbf{Y}^{(i)} = [Y^{(i)}(0), \dots, Y^{(i)}(n - 1)]$ and defined by

$$\mathbf{Y}^{(i)} = \mathbf{W}\mathbf{X}^{(i)}, \quad 1 \leq i \leq p$$

in which \mathbf{W} is the DFT matrix:

$$\mathbf{W} = \frac{1}{\sqrt{n}} \begin{bmatrix} 1 & 1 & \dots & 1 \\ 1 & \omega & \dots & \omega^{n-1} \\ \vdots & \vdots & \ddots & \vdots \\ 1 & \omega^{n-1} & \dots & \omega^{(n-1)^2} \end{bmatrix},$$

where $\omega = e^{-2\pi\sqrt{-1}/n}$.

We denote the $n \times n$ population covariance matrix of $\mathbf{X}^{(i)}$ as $\mathbf{C}^{(i,i)} = [c_{kl}^{(i,i)}]_{1 \leq k, l \leq n}$ and the $n \times n$ population cross covariance matrix between $\mathbf{X}^{(i)}$ and $\mathbf{X}^{(j)}$ as $\mathbf{C}^{(i,j)} = [c_{kl}^{(i,j)}]_{1 \leq k, l \leq n}$ for $i \neq j$. The translation invariance properties (1) and (2) imply that $\mathbf{C}^{(i,i)}$ and $\mathbf{C}^{(i,j)}$ are Toeplitz matrices. Therefore $c_{kl}^{(i,i)}$ and $c_{kl}^{(i,j)}$ depend on k and l only through the quantity $k-l$. Representing the (k, l) th entry of a Toeplitz matrix \mathbf{T} by $t(k-l)$, we write

$$c_{kl}^{(i,i)} = c^{(i,i)}(k-l) \quad \text{and} \quad c_{kl}^{(i,j)} = c^{(i,j)}(k-l),$$

where $k-l$ takes values from $1-n$ to $n-1$. In addition, $\mathbf{C}^{(i,i)}$ is symmetric.

2.2 Asymptotic Independence of Spectral Components

The following theorem states that for stationary time series, DFT components at different spectral indices (i.e. frequencies) are asymptotically uncorrelated under the condition that the auto-covariance and cross-covariance functions are absolutely summable. This theorem follows directly from the spectral theory of large Toeplitz matrices, see, for example, [14] and [15]. However, for the benefit of the reader we give a self contained proof of the theorem.

Theorem 1 Assume $\lim_{n \rightarrow \infty} \sum_{t=0}^{n-1} |c^{(i,j)}(t)| = M^{(i,j)} < \infty$ for all $1 \leq i, j \leq p$. Define $\text{err}^{(i,j)}(n) = M^{(i,j)} - \sum_{m'=0}^{n-1} |c^{(i,j)}(m')|$ and $\text{avg}^{(i,j)}(n) = \frac{1}{n} \sum_{m'=0}^{n-1} \text{err}^{(i,j)}(m')$. Then for $k \neq l$, we have:

$$\text{cor} \left(Y^{(i)}(k), Y^{(j)}(l) \right) = O(\max\{1/n, \text{avg}^{(i,j)}(n)\}).$$

In other words $Y^{(i)}(k)$ and $Y^{(j)}(l)$ are asymptotically uncorrelated as $n \rightarrow \infty$.

Proof. Without loss of generality we assume that the time series have zero mean (i.e. $\mathbb{E}[X^{(i)}(k)] = 0, 1 \leq i \leq p, 0 \leq k \leq n-1$). We first establish a representation of $\mathbb{E}[Z^{(i)}(k)Z^{(j)}(l)^*]$ for general linear functionals:

$$Z^{(i)}(k) = \sum_{m'=0}^{n-1} g_k(m') X^{(i)}(m'),$$

in which $g_k(\cdot)$ is an arbitrary complex sequence for $0 \leq k \leq n-1$. We have:

$$\begin{aligned} & \mathbb{E}[Z^{(i)}(k)Z^{(j)}(l)^*] \\ &= \mathbb{E} \left[\left(\sum_{m'=0}^{n-1} g_k(m') X^{(i)}(m') \right) \left(\sum_{n'=0}^{n-1} g_l(n') X^{(j)}(n') \right)^* \right] \\ &= \sum_{m'=0}^{n-1} g_k(m') \sum_{n'=0}^{n-1} g_l(n')^* \mathbb{E}[X^{(i)}(m') X^{(j)}(n')^*] \\ &= \sum_{m'=0}^{n-1} g_k(m') \sum_{n'=0}^{n-1} g_l(n')^* c_{m'n'}^{(i,j)} \end{aligned} \tag{3}$$

Now for a Toeplitz matrix \mathbf{T} , define the circulant matrix $\mathbf{D}_{\mathbf{T}}$ as:

$$\mathbf{D}_{\mathbf{T}} = \begin{bmatrix} t(0) & t(-1) + t(n-1) & \cdots & t(1-n) + t(1) \\ t(1) + t(1-n) & t(0) & \cdots & t(2-n) + t(2) \\ \vdots & \vdots & \ddots & \vdots \\ t(n-2) + t(-2) & t(n-3) + t(-3) & \cdots & t(-1) + t(n-1) \\ t(n-1) + t(-1) & t(n-2) + t(-2) & \cdots & t(0) \end{bmatrix}$$

We can write:

$$\mathbf{C}^{(i,j)} = \mathbf{D}_{\mathbf{C}^{(i,j)}} + \mathbf{E}^{(i,j)}$$

for some Toeplitz matrix $\mathbf{E}^{(i,j)}$. Thus $c^{(i,j)}(m' - n') = d^{(i,j)}(m' - n') + e^{(i,j)}(m' - n')$ where $d^{(i,j)}(m' - n')$ and $e^{(i,j)}(m' - n')$ are the (m', n') entries of $\mathbf{D}_{\mathbf{C}^{(i,j)}}$ and $\mathbf{E}^{(i,j)}$, respectively. Therefore, (3) can be written as:

$$\sum_{m'=0}^{n-1} g_k(m') \sum_{n'=0}^{n-1} g_l(n')^* d^{(i,j)}(m' - n') + \sum_{m'=0}^{n-1} \sum_{n'=0}^{n-1} g_k(m') g_l(n')^* e^{(i,j)}(m' - n')$$

The first term can be written as:

$$\sum_{m'=0}^{n-1} g_k(m') \left(g_l^* \otimes d^{(i,j)} \right) (m') = \sum_{m'=0}^{n-1} g_k(m') v_l^{(i,j)}(m')$$

where we have recognized $v_l^{(i,j)}(m') = g_l^* \otimes d^{(i,j)}$ as the circular convolution of $g_l^*(.)$ and $d^{(i,j)}(.)$ [16]. Let $G_k(.)$ and $D^{(i,j)}(.)$ be the the DFT of $g_k(.)$ and $d^{(i,j)}(.)$, respectively. By Plancherel's theorem [17] we have:

$$\begin{aligned} \sum_{m'=0}^{n-1} g_k(m') v_l^{(i,j)}(m') &= \sum_{m'=0}^{n-1} g_k(m') \left(v_l^{(i,j)}(m')^* \right)^* \\ &= \sum_{m'=0}^{n-1} G_k(m') \left(G_l(m') D^{(i,j)}(-m')^* \right)^* \\ &= \sum_{m'=0}^{n-1} G_k(m') G_l(m')^* D^{(i,j)}(-m'). \end{aligned} \quad (4)$$

Now let $g_k(m') = \omega^{km'}/\sqrt{n}$ for $0 \leq k, m' \leq n-1$. For this choice of $g_k(.)$ we have $G_k(m') = 0$ for all $m' \neq n-k$ and $G_k(n-k) = 1$. Hence for $k \neq l$ the quantity (4) becomes 0. Therefore using the representation $\mathbf{E}^{(i,j)} = \mathbf{C}^{(i,j)} - \mathbf{D}_{\mathbf{C}^{(i,j)}}$ we have:

$$\begin{aligned}
|\text{cov}\left(Y^{(i)}(k), Y^{(j)}(l)\right)| &= |\mathbb{E}[Y^{(i)}(k)Y^{(j)}(l)^*]| \\
&= \left| \sum_{m'=0}^{n-1} \sum_{n'=0}^{n-1} g_k(m')g_l(n')^* e^{(i,j)}(m' - n') \right| \\
&\leq \frac{1}{n} \sum_{m'=0}^{n-1} \sum_{n'=0}^{n-1} |e^{(i,j)}(m' - n')| \\
&= \frac{2}{n} \sum_{m'=0}^{n-1} m' |c^{(i,j)}(m')|, \tag{5}
\end{aligned}$$

in which the last equation is due to the fact that $|c^{(i,j)}(-m')| = |c^{(i,j)}(m')|$.

Now using (4) and (5) we obtain expressions for $\text{var}(Y^{(i)}(k))$ and $\text{var}(Y^{(j)}(l))$. Letting $j = i$ and $l = k$ in (4) and (5) gives:

$$\begin{aligned}
\text{var}\left(Y^{(i)}(k)\right) &= \text{cov}\left(Y^{(i)}(k), Y^{(i)}(k)\right) \\
&= \sum_{m'=0}^{n-1} G_k(m')G_k(m')^* D^{(i,i)}(-m') + \sum_{m'=0}^{n-1} \sum_{n'=0}^{n-1} g_k(m')g_k(n')^* e^{(i,i)}(m' - n') \\
&= n \cdot \frac{1}{\sqrt{n}} \cdot \frac{1}{\sqrt{n}} D^{(i,i)}(k) + \sum_{m'=0}^{n-1} \sum_{n'=0}^{n-1} g_k(m')g_k(n')^* e^{(i,i)}(m' - n') \\
&= D^{(i,i)}(k) + \sum_{m'=0}^{n-1} \sum_{n'=0}^{n-1} g_k(m')g_k(n')^* e^{(i,i)}(m' - n'), \tag{6}
\end{aligned}$$

in which the magnitude of the summation term is bounded as:

$$\begin{aligned}
&\left| \sum_{m'=0}^{n-1} \sum_{n'=0}^{n-1} g_k(m')g_k(n')^* e^{(i,i)}(m' - n') \right| \\
&\leq \frac{1}{n} \sum_{m'=0}^{n-1} \sum_{n'=0}^{n-1} |e^{(i,i)}(m' - n')| \\
&= \frac{2}{n} \sum_{m'=0}^{n-1} m' |c^{(i,i)}(m')|. \tag{7}
\end{aligned}$$

Similarly:

$$\text{var}\left(Y^{(j)}(l)\right) = D^{(j,j)}(l) + \sum_{m'=0}^{n-1} \sum_{n'=0}^{n-1} g_l(m')g_l(n')^* e^{(j,j)}(m' - n'), \tag{8}$$

in which

$$\begin{aligned}
& \left| \sum_{m'=0}^{n-1} \sum_{n'=0}^{n-1} g_l(m') g_l(n')^* e^{(j,j)}(m' - n') \right| \\
& \leq \frac{2}{n} \sum_{m'=0}^{n-1} m' |c^{(j,j)}(m')|. \tag{9}
\end{aligned}$$

To complete the proof the following lemma is needed.

Lemma 1 *If $\{a_{m'}\}_{m'=0}^{\infty}$ is a sequence of non-negative numbers such that $\sum_{m'=0}^{\infty} a_{m'} = M < \infty$. Define $\text{err}(n) = M - \sum_{m'=0}^{n-1} a_{m'}$ and $\text{avg}(n) = \frac{1}{n} \sum_{m'=0}^{n-1} \text{err}(m')$. Then $|\frac{1}{n} \sum_{m'=0}^{n-1} m' a_{m'}| \leq M/n + \text{err}(n) + \text{avg}(n)$.*

Proof. Let $S_0 = 0$ and for $n \geq 1$ define $S_n = \sum_{m'=0}^{n-1} a_{m'}$. We have:

$$\sum_{m'=0}^{n-1} m a_{m'} = (n-1)S_n - (S_0 + S_1 + \dots + S_{n-1}).$$

Therefore:

$$\frac{1}{n} \sum_{m'=0}^{n-1} m' a_{m'} = \frac{n-1}{n} S_{n-1} - \frac{1}{n} \sum_{m'=0}^{n-1} S_{m'}.$$

Since $M - M/n - \text{err}(n) \leq \frac{n-1}{n} S_{n-1} \leq M$ and $M - \text{avg}(n) \leq \frac{1}{n} \sum_{m'=0}^{n-1} S_{m'} \leq M$, using the triangle inequality the result follows. \square

Now let $a_{m'} = |c^{(i,j)}(m')|$. By assumption $\lim_{n \rightarrow \infty} \sum_{m'=0}^{n-1} a_{m'} = M^{(i,j)} < \infty$. Therefore, Lemma 1 along with (5) concludes:

$$\text{cov} \left(Y^{(i)}(k), Y^{(j)}(l) \right) = O(\max\{1/n, \text{err}^{(i,j)}(n), \text{avg}^{(i,j)}(n)\}). \tag{10}$$

$\text{err}^{(i,j)}(n)$ is a decreasing decreasing function of n . Therefore $\text{avg}^{(i,j)}(n) \geq \text{err}^{(i,j)}(n)$, for $n \geq 1$. Hence:

$$\text{cov} \left(Y^{(i)}(k), Y^{(j)}(l) \right) = O(\max\{1/n, \text{avg}^{(i,j)}(n)\}).$$

Similarly using Lemma 1 along with (6), (7), (8) and (9) we obtain:

$$|\text{var} \left(Y^{(i)}(k) \right) - D^{(i,i)}(k)| = O(\max\{1/n, \text{avg}^{(i,i)}(n)\}), \tag{11}$$

and

$$|\text{var} \left(Y^{(j)}(l) \right) - D^{(j,j)}(l)| = O(\max\{1/n, \text{avg}^{(j,j)}(n)\}). \tag{12}$$

Using the definition

$$\text{cor} \left(Y^{(i)}(k), Y^{(j)}(l) \right) = \frac{\text{cov} \left(Y^{(i)}(k), Y^{(j)}(l) \right)}{\sqrt{\text{var} \left(Y^{(i)}(k) \right)} \sqrt{\text{var} \left(Y^{(j)}(l) \right)}},$$

and the fact that as $n \rightarrow \infty$, $D^{(i,i)}(k)$ and $D^{(j,j)}(l)$ converge to constants $\mathbf{C}^{(i,i)}(k)$ and $\mathbf{C}^{(j,j)}(l)$, respectively, equations (10), (11) and (12) conclude:

$$\text{cor} \left(Y^{(i)}(k), Y^{(j)}(l) \right) = O(\max\{1/n, \text{avg}^{(i,j)}(n)\}).$$

□

As an example we apply Theorem 1 to a scalar auto-regressive (AR) process $X(k)$ specified by

$$X(k) = \sum_{l=1}^L \varphi_l X(k-l) + \varepsilon(k),$$

in which φ_l are real-valued coefficients and $\varepsilon(\cdot)$ is a stationary process with no temporal correlation. The auto-covariance function of an AR process can be written as [18]:

$$c(t) = \sum_{l=1}^L \alpha_l r_l^{|t|},$$

in which r_1, \dots, r_L are the roots of the polynomial $\beta(x) = x^L - \sum_{l=1}^L \varphi_l x^{L-l}$. It is known that for a stationary AR process, $|r_l| < 1$ for all $1 \leq l \leq L$ [18]. Therefore, using the definition of $\text{err}(\cdot)$ we have:

$$\begin{aligned} \text{err}(n) &= \sum_{t=n}^{\infty} |c(t)| = \sum_{t=n}^{\infty} \left| \sum_{l=1}^L \alpha_l r_l^t \right| \leq \sum_{l=1}^L |\alpha_l| \sum_{t=n}^{\infty} |r_l|^t \\ &= \sum_{l=1}^L |\alpha_l| \frac{|r_l|^n}{1 - |r_l|} \leq C \zeta^n, \end{aligned}$$

in which $C = \sum_{l=1}^L |\alpha_l|/(1 - |r_l|)$ and $\zeta = \max_{1 \leq l \leq L} |r_l| < 1$. Hence:

$$\text{avg}(n) = \frac{1}{n} \sum_{m'=0}^{n-1} \text{err}(m') \leq \frac{1}{n} \sum_{m'=0}^{n-1} C \zeta^{m'} \leq \frac{C}{n(1 - \zeta)}.$$

Therefore, Theorem 1 concludes:

$$\text{cor} (Y(k), Y(l)) = O(1/n), \quad k \neq l,$$

where $Y(\cdot)$ represents the n -point DFT of the AR process $X(\cdot)$.

In the sequel, we assume that the time series \mathbf{X} is multivariate Gaussian, i.e., $X^{(1)}, \dots, X^{(p)}$ are jointly Gaussian processes. It follows that the DFT components $Y^{(i)}(k)$ are jointly (complex) Gaussian as linear functionals of \mathbf{X} . Theorem 1 then immediately implies asymptotic independence of DFT components through a well-known property of jointly Gaussian random variables.

Corollary 1 *Assume that the time series \mathbf{X} is multivariate Gaussian. Under the absolute summability conditions in Theorem 1, the DFT components $Y^{(i)}(k)$ and $Y^{(j)}(l)$ are asymptotically independent for $k \neq l$ and $n \rightarrow \infty$.*

Corollary 1 implies that for large n , correlation analysis of the time series \mathbf{X} can be done independently on each frequency in the spectral domain. This reduces the problem of screening for hub time series to screening for hub variables among the p DFT components at a given frequency. A procedure for the latter problem and a corresponding theory are described next.

3 Complex-Valued Correlation Hub Screening

This section discusses complex-valued correlation hub screening, a generalization of real-valued correlation screening in [11, 9], for identifying highly correlated components of a complex-valued random vector from its sample values. The method is applied to multivariate time series in Section 4 to discover correlation hubs among the spectral components at each frequency. Sections 3.1 and 3.2 describe the underlying statistical model and the screening procedure. Sections 3.3 and 3.4 provide background on the U-score representation of correlation matrices and associated definitions and properties. Section 3.5 contains the main theoretical result characterizing the number of hub discoveries in the high-dimensional regime, while Section 3.6 elaborates on the phenomenon of phase transitions in the number of discoveries.

3.1 Statistical Model

We use the generic notation $\mathbf{Z} = [Z_1, Z_2, \dots, Z_p]^T$ in this section to refer to a complex-valued random vector. The mean of \mathbf{Z} is denoted as $\boldsymbol{\mu}$ and its $p \times p$ non-singular covariance matrix is denoted as $\boldsymbol{\Sigma}$. We assume that the vector \mathbf{Z} follows a complex elliptically contoured distribution with pdf $f_{\mathbf{Z}}(\mathbf{z}) = g((\mathbf{z} - \boldsymbol{\mu})^H \boldsymbol{\Sigma}^{-1}(\mathbf{z} - \boldsymbol{\mu}))$, in which $g : \mathbb{R}^{\geq 0} \rightarrow \mathbb{R}^{> 0}$ is an integrable and strictly decreasing function [19]. This assumption generalizes the Gaussian assumption made in Section 2 as the Gaussian distribution is one example of an elliptically contoured distribution.

In correlation hub screening, the quantities of interest are the correlation matrix and partial correlation matrix associated with \mathbf{Z} . These are defined as $\boldsymbol{\Gamma} = \mathbf{D}_{\boldsymbol{\Sigma}}^{-\frac{1}{2}} \boldsymbol{\Sigma} \mathbf{D}_{\boldsymbol{\Sigma}}^{-\frac{1}{2}}$ and $\boldsymbol{\Omega} = \mathbf{D}_{\boldsymbol{\Sigma}^{-1}}^{-\frac{1}{2}} \boldsymbol{\Sigma}^{-1} \mathbf{D}_{\boldsymbol{\Sigma}^{-1}}^{-\frac{1}{2}}$, respectively. Note that $\boldsymbol{\Gamma}$ and $\boldsymbol{\Omega}$ are normalized matrices with unit diagonals.

3.2 Screening Procedure

The goal of correlation hub screening is to identify highly correlated components of the random vector \mathbf{Z} from its sample realizations. Assume that m samples $\mathbf{z}_1, \dots, \mathbf{z}_m \in \mathbb{R}^p$ of \mathbf{Z} are available. To simplify the development of the

theory, the samples are assumed to be independent and identically distributed (i.i.d.) although the theory also applies to dependent samples.

We compute sample correlation and partial correlation matrices from the samples $\mathbf{z}_1, \dots, \mathbf{z}_m$ as surrogates for the unknown population correlation matrices $\mathbf{\Gamma}$ and $\mathbf{\Omega}$ in Section 3.1. First define the $p \times p$ sample covariance matrix \mathbf{S} as $\mathbf{S} = \frac{1}{m-1} \sum_{i=1}^m (\mathbf{z}_i - \bar{\mathbf{z}})(\mathbf{z}_i - \bar{\mathbf{z}})^H$, where $\bar{\mathbf{z}}$ is the sample mean, the average of $\mathbf{z}_1, \dots, \mathbf{z}_m$. The sample correlation and sample partial correlation matrices are then defined as $\mathbf{R} = \mathbf{D}_\mathbf{S}^{-\frac{1}{2}} \mathbf{S} \mathbf{D}_\mathbf{S}^{-\frac{1}{2}}$ and $\mathbf{P} = \mathbf{D}_{\mathbf{R}^\dagger}^{-\frac{1}{2}} \mathbf{R}^\dagger \mathbf{D}_{\mathbf{R}^\dagger}^{-\frac{1}{2}}$, respectively, where \mathbf{R}^\dagger is the Moore-Penrose pseudo-inverse of \mathbf{R} .

Correlation hubs are screened by applying thresholds to the sample (partial) correlation matrix. A variable Z_i is declared a hub screening discovery at degree level $\delta \in \{1, 2, \dots\}$ and threshold level $\rho \in [0, 1]$ if

$$|\{j : j \neq i, |\psi_{ij}| \geq \rho\}| \geq \delta,$$

where $\mathbf{\Psi} = \mathbf{R}$ for correlation screening and $\mathbf{\Psi} = \mathbf{P}$ for partial correlation screening. We denote by $N_{\delta, \rho} \in \{0, \dots, p\}$ the total number of hub screening discoveries at levels δ, ρ .

Correlation hub screening can also be interpreted in terms of the (*partial*) *correlation graph* $\mathcal{G}_\rho(\mathbf{\Psi})$, depicted in Fig. 1 and defined as follows. The vertices of $\mathcal{G}_\rho(\mathbf{\Psi})$ are v_1, \dots, v_p which correspond to Z_1, \dots, Z_p , respectively. For $1 \leq i, j \leq p$, v_i and v_j are connected by an edge in $\mathcal{G}_\rho(\mathbf{\Psi})$ if the magnitude of the sample (partial) correlation coefficient between Z_i and Z_j is at least ρ . A vertex of $\mathcal{G}_\rho(\mathbf{\Psi})$ is called a δ -hub if its degree, the number of incident edges, is at least δ . Then the number of discoveries $N_{\delta, \rho}$ defined earlier is the number of δ -hubs in the graph $\mathcal{G}_\rho(\mathbf{\Psi})$.

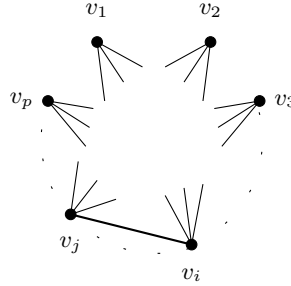


Fig. 1. Complex-valued (partial) correlation hub screening thresholds the sample correlation or partial correlation matrix, denoted generically by the matrix $\mathbf{\Psi}$, to find variables Z_i that are highly correlated with other variables. This is equivalent to finding hubs in a graph $\mathcal{G}_\rho(\mathbf{\Psi})$ with p vertices v_1, \dots, v_p . For $1 \leq i, j \leq p$, v_i is connected to v_j in $\mathcal{G}_\rho(\mathbf{\Psi})$ if $|\psi_{ij}| \geq \rho$.

3.3 U-score Representation of Correlation Matrices

Our theory for complex-valued correlation screening is based on the U-score representation of the sample correlation and partial correlation matrices. Similarly to the real case [9], it can be shown that there exists an $(m-1) \times p$ complex-valued matrix $\mathbb{U}_{\mathbf{R}}$ with unit-norm columns $\mathbf{u}_{\mathbf{R}}^{(i)} \in \mathbb{C}^{m-1}$ such that the following representation holds:

$$\mathbf{R} = \mathbb{U}_{\mathbf{R}}^H \mathbb{U}_{\mathbf{R}}. \quad (13)$$

Similar to Lemma 1 in [9] it is straightforward to show that:

$$\mathbf{R}^\dagger = \mathbb{U}_{\mathbf{R}}^H (\mathbb{U}_{\mathbf{R}} \mathbb{U}_{\mathbf{R}}^H)^{-2} \mathbb{U}_{\mathbf{R}}.$$

Hence by defining $\mathbb{U}_{\mathbf{P}} = (\mathbb{U}_{\mathbf{R}} \mathbb{U}_{\mathbf{R}}^H)^{-1} \mathbb{U}_{\mathbf{R}} \mathbf{D}_{\mathbb{U}_{\mathbf{R}}^H (\mathbb{U}_{\mathbf{R}} \mathbb{U}_{\mathbf{R}}^H)^{-2} \mathbb{U}_{\mathbf{R}}}^{-\frac{1}{2}}$ we have the representation:

$$\mathbf{P} = \mathbb{U}_{\mathbf{P}}^H \mathbb{U}_{\mathbf{P}}, \quad (14)$$

where the $(m-1) \times p$ matrix $\mathbb{U}_{\mathbf{P}}$ has unit-norm columns $\mathbf{u}_{\mathbf{P}}^{(i)} \in \mathbb{C}^{m-1}$.

3.4 Properties of U-scores

The U-score factorizations in (13) and (14) show that sample (partial) correlation matrices can be represented in terms of unit vectors in \mathbb{C}^{m-1} . This subsection presents definitions and properties related to U-scores that will be used in Section 3.5.

We denote the unit spheres in \mathbb{R}^{m-1} and \mathbb{C}^{m-1} as S_{m-1} and T_{m-1} , respectively. The surface areas of S_{m-1} and T_{m-1} are denoted as a_{m-1} and b_{m-1} respectively. Define the interleaving function $h : \mathbb{R}^{2m-2} \rightarrow \mathbb{C}^{m-1}$ as below:

$$h([x_1, x_2, \dots, x_{2m-2}]^T) = [x_1 + x_2\sqrt{-1}, x_3 + x_4\sqrt{-1}, \dots, x_{2m-3} + x_{2m-2}\sqrt{-1}]^T.$$

Note that $h(\cdot)$ is a one-to-one and onto function and it maps S_{2m-2} to T_{m-1} .

For a fixed vector $\mathbf{u} \in T_{m-1}$ and a threshold $0 \leq \rho \leq 1$ define the spherical cap in T_{m-1} :

$$A_\rho(\mathbf{u}) = \{\mathbf{y} : \mathbf{y} \in T_{m-1}, |\mathbf{y}^H \mathbf{u}| \geq \rho\}.$$

Also define P_0 as the probability that a random point \mathbf{Y} that is uniformly distributed on T_{m-1} falls into $A_\rho(\mathbf{u})$. Below we give a simple expression for P_0 as a function of ρ and m .

Lemma 2 *Let \mathbf{Y} be an $(m-1)$ -dimensional complex-valued random vector that is uniformly distributed over T_{m-1} . We have $P_0 = \mathbb{P}(\mathbf{Y} \in A_\rho(\mathbf{u})) = (1 - \rho^2)^{m-2}$.*

Proof. Without loss of generality we assume $\mathbf{u} = [1, 0, \dots, 0]^T$. We have:

$$P_0 = \mathbb{P}(|Y_1| \geq \rho) = \mathbb{P}(\Re(Y_1)^2 + \Im(Y_1)^2 \geq \rho^2).$$

Since \mathbf{Y} is uniform on T_{m-1} , we can write $\mathbf{Y} = \mathbf{X}/\|\mathbf{X}\|_2$, in which \mathbf{X} is complex-valued random vector whose entries are i.i.d. complex-valued Gaussian variables with mean 0 and variance 1. Thus:

$$\begin{aligned} P_0 &= \mathbb{P}((\Re(X_1)^2 + \Im(X_1)^2) / \|\mathbf{X}\|_2^2 \geq \rho^2) \\ &= \mathbb{P}\left((1 - \rho^2)(\Re(X_1)^2 + \Im(X_1)^2) \geq \rho^2 \sum_{k=2}^{m-1} \Re(X_k)^2 + \Im(X_k)^2\right). \end{aligned}$$

Define $V_1 = \Re(X_1)^2 + \Im(X_1)^2$ and $V_2 = \sum_{k=2}^{m-1} \Re(X_k)^2 + \Im(X_k)^2$. V_1 and V_2 are independent and have chi-squared distributions with 2 and $2(m-2)$ degrees of freedom, respectively [20]. Therefore,

$$\begin{aligned} P_0 &= \int_0^\infty \int_{\rho^2 v_2 / (1-\rho^2)}^\infty \chi_{2(m-2)}^2(v_2) \chi_2^2(v_1) dv_1 dv_2 \\ &= \int_0^\infty \chi_{2(m-2)}^2(v_2) \int_{\rho^2 v_2 / (1-\rho^2)}^\infty \frac{1}{2} e^{-v_1/2} dv_1 dv_2 \\ &= \int_0^\infty \frac{1}{2^{m-2} \Gamma(m-2)} v_2^{m-3} e^{-v_2/2} e^{-\frac{\rho^2}{2(1-\rho^2)} v_2} dv_2 \\ &= \frac{1}{\Gamma(m-2)} (1-\rho^2)^{m-2} \int_0^\infty x^{m-3} e^{-x} dx \\ &= \frac{1}{\Gamma(m-2)} (1-\rho^2)^{m-2} \Gamma(m-2) = (1-\rho^2)^{m-2}, \end{aligned}$$

in which we have made a change of variable $x = \frac{v_2}{2(1-\rho^2)}$. \square

Under the assumption that the joint pdf of \mathbf{Z} exists, the p columns of the U-score matrix have joint pdf $f_{\mathbf{U}_1, \dots, \mathbf{U}_p}(\mathbf{u}_1, \dots, \mathbf{u}_p)$ on $T_{m-1}^p = \times_{i=1}^p T_{m-1}$. The following $(\delta+1)$ -fold average of the joint pdf will play a significant role in Section 3.5. This $(\delta+1)$ -fold average is defined as:

$$\begin{aligned} \overline{f_{\mathbf{U}_{*1}, \dots, \mathbf{U}_{*\delta+1}}}(\mathbf{u}_1, \dots, \mathbf{u}_{\delta+1}) &= \frac{1}{(2\pi)^{\delta+1} p^{\binom{p-1}{\delta}}} \times \\ &\sum_{1 \leq i_1 < \dots < i_\delta \leq p, i_{\delta+1} \notin \{i_1, \dots, i_\delta\}} \int_0^{2\pi} \int_0^{2\pi} \dots \int_0^{2\pi} \\ &f_{\mathbf{U}_{i_1}, \dots, \mathbf{U}_{i_\delta}, \mathbf{U}_{i_{\delta+1}}} (e^{\sqrt{-1}\theta_1} \mathbf{u}_1, \dots, e^{\sqrt{-1}\theta_\delta} \mathbf{u}_\delta, e^{\sqrt{-1}\theta_{\delta+1}} \mathbf{u}_{\delta+1}) d\theta_1 \dots d\theta_\delta d\theta. \end{aligned}$$

Also for a joint pdf $f_{\mathbf{U}_1, \dots, \mathbf{U}_{\delta+1}}(\mathbf{u}_1, \dots, \mathbf{u}_{\delta+1})$ on $T_{m-1}^{\delta+1}$ define

$$J(f_{\mathbf{U}_1, \dots, \mathbf{U}_{\delta+1}}) = a_{2m-2}^\delta \int_{S_{2m-2}} f_{\mathbf{U}_1, \dots, \mathbf{U}_{\delta+1}}(h(\mathbf{u}), \dots, h(\mathbf{u})) d\mathbf{u}.$$

Note that $J(f_{\mathbf{U}_1, \dots, \mathbf{U}_{\delta+1}})$ is proportional to the integral of $f_{\mathbf{U}_1, \dots, \mathbf{U}_{\delta+1}}$ over the manifold $\mathbf{u}_1 = \dots = \mathbf{u}_{\delta+1}$. The quantity $J(\overline{f_{\mathbf{U}_{*1}, \dots, \mathbf{U}_{*(\delta+1)}}})$ is key in determining the asymptotic average number of hubs in a complex-valued correlation network. This will be described in more detail in Sec. 3.5.

Let $\mathbf{i} = (i_0, i_1, \dots, i_\delta)$ be a set of distinct indices, i.e., $1 \leq i_0 \leq p, 1 \leq i_1 < \dots < i_\delta \leq p$ and $i_1, \dots, i_\delta \neq i_0$. For a U-score matrix \mathbb{U} define the dependency coefficient between the columns $\mathbf{U}_{\mathbf{i}} = \{\mathbf{U}_{i_0}, \mathbf{U}_{i_1}, \dots, \mathbf{U}_{i_\delta}\}$ and their complementary k -NN (k -nearest neighbor) set $A_k(\mathbf{i})$ defined in (29) and Fig. 2 as

$$\Delta_{p,m,k,\delta}(\mathbf{i}) = \left\| (f_{\mathbf{U}_{\mathbf{i}}|\mathbf{U}_{A_k(\mathbf{i})}} - f_{\mathbf{U}_{\mathbf{i}}}) / f_{\mathbf{U}_{\mathbf{i}}} \right\|_\infty,$$

where $\|\cdot\|_\infty$ denotes the supremum norm. The average of these coefficients is defined as:

$$\|\Delta_{p,m,k,\delta}\|_1 = \frac{1}{p \binom{p-1}{\delta}} \sum_{i_0=1}^p \sum_{\substack{i_1, \dots, i_\delta \neq i_0 \\ 1 \leq i_1 < \dots < i_\delta \leq p}} \Delta_{p,m,k,\delta}(\mathbf{i}). \quad (15)$$

3.5 Number of Hub Discoveries in the High-Dimensional Limit

We now present the main theoretical result on complex-valued correlation screening. The following theorem gives asymptotic expressions for the mean number of δ -hubs and the probability of discovery of at least one δ -hub in the graph $\mathcal{G}_\rho(\Psi)$. It also gives bounds on the rates of convergence to these approximations as the dimension p increases and $\rho \rightarrow 1$. We use $\mathbb{U} = [\mathbf{U}_1, \dots, \mathbf{U}_p]$ as a generic notation for the U-score representation of the sample (partial) correlation matrix. The asymptotic expression for the mean $\mathbb{E}[N_{\delta,\rho}]$ is denoted by Λ and is given by:

$$\Lambda = p \binom{p-1}{\delta} P_0^\delta J(\overline{f_{\mathbf{U}_{*1}, \dots, \mathbf{U}_{*(\delta+1)}}}). \quad (16)$$

Define $\eta_{p,\delta}$ as:

$$\eta_{p,\delta} = p^{1/\delta} (p-1) P_0 = p^{1/\delta} (p-1) (1-\rho^2)^{(m-2)}, \quad (17)$$

where the last equation is due to Lemma 2. The parameter k below represents an upper bound on the true hub degree, i.e. the number of non-zero entries in any row of the population covariance matrix Σ . Also let $\varphi(\delta)$ be the function that takes values $\varphi(\delta) = 2$ for $\delta = 1$ and $\varphi(\delta) = 1$ for $\delta > 1$.

Theorem 2 *Let $\mathbb{U} = [\mathbf{U}_1, \dots, \mathbf{U}_p]$ be a $(m-1) \times p$ random matrix with $\mathbf{U}_i \in T_{m-1}$ where $m > 2$. Let $\delta \geq 1$ be a fixed integer. Assume the joint pdf of any subset of the \mathbf{U}_i 's is bounded and differentiable. Then, with Λ defined in (16),*

$$|\mathbb{E}[N_{\delta,\rho}] - \Lambda| \leq O\left(\eta_{p,\delta}^\delta \max\left\{\eta_{p,\delta} p^{-1/\delta}, (1-\rho)^{1/2}\right\}\right). \quad (18)$$

Furthermore, let $N_{\delta,\rho}^*$ be a Poisson distributed random variable with rate $\mathbb{E}[N_{\delta,\rho}^*] = \Lambda/\varphi(\delta)$. If $(p-1)P_0 \leq 1$, then

$$\begin{aligned} & |\mathbb{P}(N_{\delta,\rho} > 0) - \mathbb{P}(N_{\delta,\rho}^* > 0)| \leq \\ & \begin{cases} O\left(\eta_{p,\delta}^\delta \max\left\{\eta_{p,\delta}^\delta (k/p)^{\delta+1}, Q_{p,k,\delta}, \|\Delta_{p,m,k,\delta}\|_1, p^{-1/\delta}, (1-\rho)^{1/2}\right\}\right), & \delta > 1 \\ O\left(\eta_{p,1} \max\left\{\eta_{p,1} (k/p)^2, \|\Delta_{p,m,k,1}\|_1, p^{-1}, (1-\rho)^{1/2}\right\}\right), & \delta = 1 \end{cases}, \end{aligned} \quad (19)$$

with $Q_{p,k,\delta} = \eta_{p,\delta} (k/p^{1/\delta})^{\delta+1}$ and $\|\Delta_{p,m,k,\delta}\|_1$ defined in (15).

Proof. The proof is similar to the proof of proposition 1 in [9]. First we prove (18). Let $\phi_i = I(d_i \geq \delta)$ be the indicator of the event that $d_i \geq \delta$, in which d_i represents the degree of the vertex v_i in the graph $\mathcal{G}_\rho(\Psi)$. We have $N_{\delta,\rho} = \sum_{i=1}^p \phi_i$. With ϕ_{ij} being the indicator of the presence of an edge in $\mathcal{G}_\rho(\Psi)$ between vertices v_i and v_j we have the relation:

$$\phi_i = \sum_{l=\delta}^{p-1} \sum_{\mathbf{k} \in \check{\mathcal{C}}_i(p-1,l)} \prod_{j=1}^l \phi_{ik_j} \prod_{q=l+1}^{p-1} (1 - \phi_{ik_q}) \quad (20)$$

where we have defined the index vector $\mathbf{k} = (k_1, \dots, k_{p-1})$ and the set

$$\check{\mathcal{C}}_i(p-1, l) =$$

$$\{\mathbf{k} : k_1 < \dots < k_l, k_{l+1} < \dots < k_{p-1} \mid k_j \in \{1, \dots, p\} - \{i\}, k_j \neq k_{j'}\}.$$

The inner summation in (20) simply sums over the set of distinct indices not equal to i that index all $\binom{p-1}{l}$ different types of products of the form: $\prod_{j=1}^l \phi_{ik_j} \prod_{q=l+1}^{p-1} (1 - \phi_{ik_q})$. Subtracting $\sum_{\mathbf{k} \in \check{\mathcal{C}}_i(p-1,\delta)} \prod_{j=1}^\delta \phi_{ik_j}$ from both sides of (20)

$$\begin{aligned} & \phi_i - \sum_{\mathbf{k} \in \check{\mathcal{C}}_i(p-1,\delta)} \prod_{j=1}^\delta \phi_{ik_j} \\ &= \sum_{l=\delta+1}^{p-1} \sum_{\mathbf{k} \in \check{\mathcal{C}}_i(p-1,l)} \prod_{j=1}^l \phi_{ik_j} \prod_{q=l+1}^{p-1} (1 - \phi_{ik_q}) \\ &+ \sum_{\mathbf{k} \in \check{\mathcal{C}}_i(p-1,l)} \sum_{q=\delta+1}^{p-1} (-1)^{q-\delta} \\ & \sum_{k'_{\delta+1} < \dots < k'_q, \{k'_{\delta+1}, \dots, k'_q\} \subset \{k_{\delta+1}, \dots, k_{p-1}\}} \prod_{j=1}^l \phi_{ik_j} \prod_{s=\delta+1}^q \phi_{ik'_s} \end{aligned} \quad (21)$$

in which we have used the expansion

$$\prod_{q=\delta+1}^{p-1} (1 - \phi_{ik_q}) = 1 + \sum_{q=\delta+1}^{p-1} (-1)^{q-\delta} \sum_{k'_{\delta+1} < \dots < k'_q, \{k'_{\delta+1}, \dots, k'_q\} \subset \{k_{\delta+1}, \dots, k_{p-1}\}} \prod_{s=\delta+1}^q \phi_{ik'_s}.$$

The following simple asymptotic representation will be useful in the sequel. For any $i_1, \dots, i_k \in \{1, \dots, p\}$, $i_1 \neq \dots \neq i_k \neq i$, $k \in \{1, \dots, p-1\}$,

$$\begin{aligned} \mathbb{E} \left[\prod_{j=1}^k \phi_{ii_j} \right] &= \int_{S_{2m-2}} \int_{h^{-1}(A_\rho(\mathbf{v}))} \dots \int_{h^{-1}(A_\rho(\mathbf{v}))} \\ &\quad f_{\mathbf{U}_{i_1}, \dots, \mathbf{U}_{i_k}, \mathbf{U}_i}(h(\mathbf{v}_1), \dots, h(\mathbf{v}_k), h(\mathbf{v})) d\mathbf{v}_1 \dots d\mathbf{v}_k d\mathbf{v} \\ &\leq P_0^k a_{2m-2}^k M_{k|1} \end{aligned} \quad (22)$$

where $P_0, A_\rho(\mathbf{u})$ and the function $h(\cdot)$ are defined in Sec. 3.4. Moreover

$$M_{k|1} = \max_{i_1 \neq \dots \neq i_{k+1}} \left\| f_{\mathbf{U}_{i_1}, \dots, \mathbf{U}_{i_k} | \mathbf{U}_{i_{k+1}}} \right\|_\infty.$$

The following simple generalization of (22) to arbitrary product indices ϕ_{ij} will also be needed

$$\mathbb{E} \left[\prod_{l=1}^q \phi_{i_l j_l} \right] \leq P_0^q a_{2m-2}^q M_{|Q|}, \quad (23)$$

where $Q = \text{unique}(\{i_l, j_l\}_{l=1}^q)$ is the set of unique indices among the distinct pairs $\{(i_l, j_l)\}_{l=1}^q$ and $M_{|Q|}$ is a bound on the joint pdf of \mathbf{U}_Q .

Define the random variable

$$\theta_i = \binom{p-1}{\delta}^{-1} \sum_{\mathbf{k} \in \check{C}_i(p-1, \delta)} \prod_{j=1}^{\delta} \phi_{ik_j}.$$

We show below that for sufficiently large p

$$\left| \mathbb{E}[\phi_i] - \binom{p-1}{\delta} \mathbb{E}[\theta_i] \right| \leq \gamma_{p, \delta} ((p-1)P_0)^{\delta+1}, \quad (24)$$

where $\gamma_{p, \delta} = \max_{\delta+1 \leq l < p} \{a_{2m-2}^l M_{l|1}\} \left(e - \sum_{l=0}^{\delta} \frac{1}{l!} \right) (1 + (\delta!)^{-1})$ and $M_{l|1}$ is a least upper bound on any l -dimensional joint pdf of the variables $\{\mathbf{U}_i\}_{j \neq i}^p$ conditioned on \mathbf{U}_i .

To show inequality (24) take expectations of (21) and apply the bound (22) to obtain

$$\begin{aligned} &\left| \mathbb{E}[\phi_i] - \binom{p-1}{\delta} \mathbb{E}[\theta_i] \right| \leq \\ &\left| \sum_{l=\delta+1}^{p-1} \binom{p-1}{l} P_0^l a_{2m-2}^l M_{l|1} + \binom{p-1}{\delta} \sum_{l=1}^{p-1-\delta} \binom{p-1-\delta}{l} P_0^{\delta+l} a_{2m-2}^{\delta+l} M_{\delta+l|1} \right| \\ &\leq A(1 + (\delta!)^{-1}), \end{aligned} \quad (25)$$

where

$$A = \sum_{l=\delta+1}^{p-1} \binom{p-1}{l} ((p-1)P_0)^l a_{2m-2}^l M_{l|1}.$$

The line (25) follows from the identity $\binom{p-1-\delta}{l} \binom{p-1}{\delta} = \binom{p-1}{l+\delta} \binom{l+\delta}{l}$ and a change of index in the second summation on the previous line. Since $(p-1)P_0 < 1$

$$\begin{aligned} |A| &\leq \max_{\delta+1 \leq l < p} \{a_{2m-2}^l M_{l|1}\} \sum_{l=\delta+1}^{p-1} \binom{p-1}{l} ((p-1)P_0)^l \\ &\leq \max_{\delta+1 \leq l < p} \{a_{2m-2}^l M_{l|1}\} \left(e - \sum_{l=0}^{\delta} \frac{1}{l!} \right) ((p-1)P_0)^{\delta+1}. \end{aligned}$$

Application of the mean value theorem to the integral representation (22) yields

$$|\mathbb{E}[\theta_i] - P_0^\delta J(\overline{f_{\mathbf{U}_{*1-i}, \dots, \mathbf{U}_{*\delta-i}, \mathbf{U}_i}})| \leq \tilde{\gamma}_{p,\delta} ((p-1)P_0)^\delta r, \quad (26)$$

where

$$\begin{aligned} &\overline{f_{\mathbf{U}_{*1-i}, \dots, \mathbf{U}_{*\delta-i}, \mathbf{U}_i}}(\mathbf{u}_1, \dots, \mathbf{u}_{\delta+1}) = \\ &\quad \frac{1}{(2\pi)^\delta \binom{p-1}{\delta}} \sum_{\substack{1 \leq i_1 < \dots < i_\delta \leq p \\ i \notin \{i_1, \dots, i_\delta\}}} \int_0^{2\pi} \dots \int_0^{2\pi} \\ &\quad f_{\mathbf{U}_{i_1}, \dots, \mathbf{U}_{i_\delta}, \mathbf{U}_i}(e^{\sqrt{-1}\theta_1} \mathbf{u}_1, \dots, e^{\sqrt{-1}\theta_\delta} \mathbf{u}_\delta, \mathbf{u}_{\delta+1}) d\theta_1 \dots d\theta_\delta, \end{aligned}$$

$r = \sqrt{2(1-\rho)}$, $\tilde{\gamma}_{p,\delta} = 2a_{2m-2}^{\delta+1} \dot{M}_{\delta+1|1}/\delta!$ and $\dot{M}_{\delta+1|1}$ is a bound on the norm of the gradient

$$\nabla_{\mathbf{u}_{i_1}, \dots, \mathbf{u}_{i_\delta}} \overline{f_{\mathbf{U}_{*1-i}, \dots, \mathbf{U}_{*\delta-i}, \mathbf{U}_i}}(\mathbf{u}_{i_1}, \dots, \mathbf{u}_{i_\delta} | \mathbf{u}_i).$$

Combining (24)-(26) and the relation $r = O((1-\rho)^{1/2})$,

$$\begin{aligned} &\left| \mathbb{E}[\phi_i] - \binom{p-1}{\delta} P_0^\delta J(\overline{f_{\mathbf{U}_{*1}, \dots, \mathbf{U}_{*(\delta+1)}}}) \right| \\ &\leq O\left(((p-1)P_0)^\delta \max \left\{ (p-1)P_0, (1-\rho)^{1/2} \right\} \right). \end{aligned}$$

Summing over i and recalling the definitions (16) and (17) of Λ and $\eta_{p,\delta}$,

$$\begin{aligned} |\mathbb{E}[N_{\delta,\rho}] - \Lambda| &\leq O\left(p((p-1)P_0)^\delta \max \left\{ (p-1)P_0, (1-\rho)^{1/2} \right\} \right) \\ &= O\left(\eta_{p,\delta}^\delta \max \left\{ \eta_{p,\delta} p^{-1/\delta}, (1-\rho)^{1/2} \right\} \right). \end{aligned}$$

This establishes the bound (18).

Next we prove the bound (19) by using the Chen-Stein method [21]. Define:

$$\tilde{N}_{\delta,\rho} = \frac{1}{\varphi(\delta)} \sum_{i_0=1}^p \sum_{1 \leq i_1 < \dots < i_\delta \leq p} \prod_{j=1}^{\delta} \phi_{i_0 i_j}, \quad (27)$$

Where the second sum is over the indices $1 \leq i_1 < \dots < i_\delta \leq p$ such that $i_j \neq i_0, 1 \leq j \leq \delta$. For $\mathbf{i} \stackrel{\text{def}}{=} (i_0, i_1, \dots, i_\delta)$ define the index set $B_{\mathbf{i}} = B_{i_0, i_1, \dots, i_\delta} = \{(j_0, j_1, \dots, j_\delta) : j_l \in \mathcal{N}_k(i_l) \cup \{i_l\}, l = 0, \dots, \delta\} \cap \mathcal{C}^<$ where $\mathcal{C}^< = \{(j_0, \dots, j_\delta) : 1 \leq j_0 \leq p, 1 \leq j_1 < \dots < j_\delta \leq p, j_l \neq j_0, 1 \leq l \leq \delta\}$. These index the distinct sets of points $\mathbf{U}_{\mathbf{i}} = \{\mathbf{U}_{i_0}, \mathbf{U}_{i_1}, \dots, \mathbf{U}_{i_\delta}\}$ and their respective k -NN's. Note that $|B_{\mathbf{i}}| \leq k^{\delta+1}$. Identifying $\tilde{N}_{\delta,\rho} = \sum_{\mathbf{i} \in \mathcal{C}^<} \prod_{l=1}^{\delta} \phi_{i_0 i_l}$ and $N_{\delta,\rho}^*$ a Poisson distributed random variable with rate $\mathbb{E}[\tilde{N}_{\delta,\rho}]$, the Chen-Stein bound [21, Theorem 1] is

$$2 \max_A |\mathbb{P}(\tilde{N}_{\delta,\rho} \in A) - \mathbb{P}(N_{\delta,\rho}^* \in A)| \leq b_1 + b_2 + b_3, \quad (28)$$

where

$$b_1 = \sum_{\mathbf{i} \in \mathcal{C}^<} \sum_{\mathbf{j} \in B_{\mathbf{i}}} \mathbb{E} \left[\prod_{l=1}^{\delta} \phi_{i_0 i_l} \right] \mathbb{E} \left[\prod_{q=1}^{\delta} \phi_{j_0 j_q} \right],$$

$$b_2 = \sum_{\mathbf{i} \in \mathcal{C}^<} \sum_{\mathbf{j} \in B_{\mathbf{i} - \{\mathbf{i}\}}} \mathbb{E} \left[\prod_{l=1}^{\delta} \phi_{i_0 i_l} \prod_{q=1}^{\delta} \phi_{j_0 j_q} \right],$$

and, for $p_{\mathbf{i}} = \mathbb{E}[\prod_{l=1}^{\delta} \phi_{i_0 i_l}]$,

$$b_3 = \sum_{\mathbf{i} \in \mathcal{C}^<} \mathbb{E} \left[\mathbb{E} \left[\prod_{l=1}^{\delta} \phi_{i_0 i_l} - p_{\mathbf{i}} \middle| \phi_{\mathbf{j}} : \mathbf{j} \notin B_{\mathbf{i}} \right] \right].$$

Over the range of indices in the sum of b_1 $\mathbb{E}[\prod_{l=1}^{\delta} \phi_{i_0 i_l}]$ is of order $O(P_0^\delta)$, by (23), and therefore

$$b_1 \leq O(p^{\delta+1} k^{\delta+1} P_0^{2\delta}) = O(\eta_{p,\delta}^{2\delta} (k/p)^{\delta+1}),$$

which follows from definition (17). More care is needed to bound b_2 due to the repetition of characteristic functions ϕ_{ij} . Since $\mathbf{i} \neq \mathbf{j}$, $\mathbb{E}[\prod_{l=1}^{\delta} \phi_{i_0 i_l} \prod_{q=1}^{\delta} \phi_{j_0 j_q}]$ is a multiplication of at least $\delta + 1$ different characteristic functions, hence by (23),

$$\mathbb{E}[\prod_{l=1}^{\delta} \phi_{i_0 i_l} \prod_{q=1}^{\delta} \phi_{j_0 j_q}] = O(P_0^{\delta+1}).$$

Therefore, we conclude that

$$b_2 \leq O(p^{\delta+1} k^{\delta+1} P_0^{\delta+1}).$$

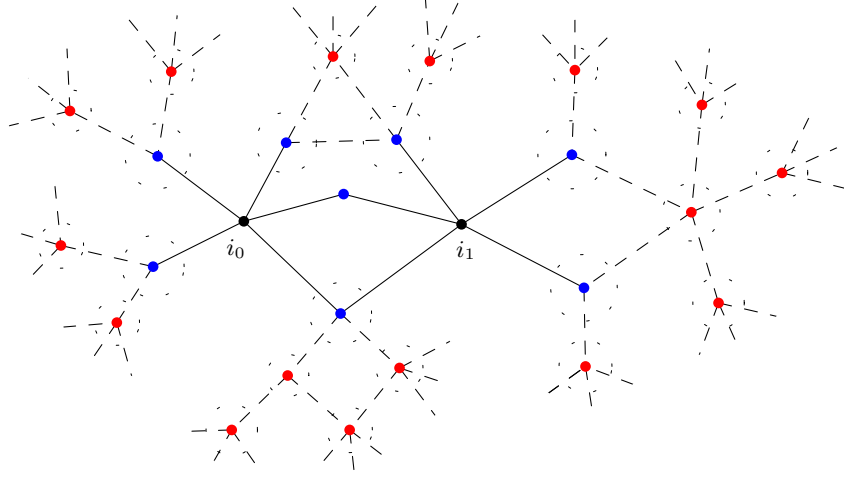


Fig. 2. The complementary k -NN set $A_k(\mathbf{i})$ illustrated for $\delta = 1$ and $k = 5$. Here we have $\mathbf{i} = (i_0, i_1)$. The vertices i_0, i_1 and their k -NNs are depicted in black and blue respectively. The complement of the union of $\{i_0, i_1\}$ and its k -NNs is the complementary k -NN set $A_k(\mathbf{i})$ and is depicted in red.

Next we bound the term b_3 in (28). The set

$$A_k(\mathbf{i}) = B_{\mathbf{i}}^c - \{\mathbf{i}\} \quad (29)$$

indexes the complementary k -NN of $\mathbf{U}_{\mathbf{i}}$ (see Fig. 2) so that, using the representation (23),

$$\begin{aligned} b_3 &= \sum_{\mathbf{i} \in \mathcal{C}^<} \mathbb{E} \left[\mathbb{E} \left[\prod_{l=1}^{\delta} \phi_{i_0 i_l} - p_{\mathbf{i}} \middle| \mathbf{U}_{A_k(\mathbf{i})} \right] \right] \\ &= \sum_{\mathbf{i} \in \mathcal{C}^<} \int_{S_{2m-2}^{|A_k(\mathbf{i})|}} d\mathbf{u}_{A_k(\mathbf{i})} \left(\prod_{l=1}^{\delta} \int_{S_{2m-2}} d\mathbf{u}_{i_0} \int_{A(r, \mathbf{u}_{i_0})} d\mathbf{u}_{i_l} \right) \\ &\quad \left(\frac{f_{\mathbf{U}_{\mathbf{i}}|\mathbf{U}_{A_k}}(\mathbf{u}_{\mathbf{i}}|\mathbf{u}_{A_k(\mathbf{i})}) - f_{\mathbf{U}_{\mathbf{i}}}(\mathbf{u}_{\mathbf{i}})}{f_{\mathbf{U}_{\mathbf{i}}}(\mathbf{u}_{\mathbf{i}})} \right) f_{\mathbf{U}_{\mathbf{i}}}(\mathbf{u}_{\mathbf{i}}) f_{\mathbf{U}_{A_k(\mathbf{i})}}(\mathbf{u}_{A_k(\mathbf{i})}) \\ &\leq O(p^{\delta+1} P_0^{\delta} \|\Delta_{p,m,k,\delta}\|_1) = O(\eta_{p,\delta}^{\delta} \|\Delta_{p,m,k,\delta}\|_1). \end{aligned}$$

Note that by definition of $\tilde{N}_{\delta,\rho}$ we have $\tilde{N}_{\delta,\rho} > 0$ if and only if $N_{\delta,\rho} > 0$. This yields:

$$\begin{aligned}
& \left| \mathbb{P}(N_{\delta,\rho} > 0) - (1 - \exp(-\Lambda)) \right| \leq \left| \mathbb{P}(\tilde{N}_{\delta,\rho} > 0) - \mathbb{P}(N_{\delta,\rho} > 0) \right| + \\
& \left| \mathbb{P}(\tilde{N}_{\delta,\rho} > 0) - \left(1 - \exp(-\mathbb{E}[\tilde{N}_{\delta,\rho}]) \right) \right| + \left| \exp(-\mathbb{E}[\tilde{N}_{\delta,\rho}]) - \exp(-\Lambda) \right| \\
& \leq b_1 + b_2 + b_3 + O\left(\left|\mathbb{E}[\tilde{N}_{\delta,\rho}] - \Lambda\right|\right)
\end{aligned} \tag{30}$$

Combining the above inequalities on b_1 , b_2 and b_3 yields the first three terms in the argument of the “max” on the right side of (19).

It remains to bound the term $|\mathbb{E}[\tilde{N}_{\delta,\rho}] - \Lambda|$. Application of the mean value theorem to the multiple integral (23) gives

$$\left| \mathbb{E} \left[\prod_{l=1}^{\delta} \phi_{iil} \right] - P_0^{\delta} J \left(f_{\mathbf{U}_{i_1}, \dots, \mathbf{U}_{i_{\delta}}, \mathbf{U}_i} \right) \right| \leq O(P_0^{\delta} r).$$

Applying relation (27) yields

$$\left| \mathbb{E}[\tilde{N}_{\delta,\rho}] - p \binom{p-1}{\delta} P_0^{\delta} J \left(\overline{f_{\mathbf{U}_{*1}, \dots, \mathbf{U}_{*(\delta+1)}}} \right) \right| \leq O(p^{\delta+1} P_0^{\delta} r) = O(\eta_{p,\delta}^{\delta} r).$$

Combine this with (30) to obtain the bound (19). This completes the proof of Theorem 2. \square

An immediate consequence of Theorem 2 is the following result, similar to Proposition 2 in [9], which provides asymptotic expressions for the mean number of δ -hubs and the probability of the event $N_{\delta,\rho} > 0$ as p goes to ∞ and ρ converges to 1 at a prescribed rate.

Corollary 2 *Let $\rho_p \in [0, 1]$ be a sequence converging to one as $p \rightarrow \infty$ such that $\eta_{p,\delta} = p^{1/\delta}(p-1)(1-\rho_p^2)^{(m-2)} \rightarrow e_{m,\delta} \in (0, \infty)$. Then*

$$\lim_{p \rightarrow \infty} \mathbb{E}[N_{\delta,\rho_p}] = \Lambda_{\infty} = e_{m,\delta}^{\delta} / \delta! \lim_{p \rightarrow \infty} J(\overline{f_{\mathbf{U}_{*1}, \dots, \mathbf{U}_{*(\delta+1)}}}). \tag{31}$$

Assume that $k = o(p^{1/\delta})$ and that for the weak dependency coefficient $\|\Delta_{p,m,k,\delta}\|_1$, defined via (15), we have $\lim_{p \rightarrow \infty} \|\Delta_{p,m,k,\delta}\|_1 = 0$. Then

$$\mathbb{P}(N_{\delta,\rho_p} > 0) \rightarrow 1 - \exp(-\Lambda_{\infty}/\varphi(\delta)). \tag{32}$$

Corollary 2 shows that in the limit $p \rightarrow \infty$, the number of detected hubs depends on the true population correlations only through the quantity $J(\overline{f_{\mathbf{U}_{*1}, \dots, \mathbf{U}_{*(\delta+1)}}})$. In some cases $J(\overline{f_{\mathbf{U}_{*1}, \dots, \mathbf{U}_{*(\delta+1)}}})$ can be evaluated explicitly. Similar to the argument in [9], it can be shown that if the population covariance matrix Σ is sparse in the sense that its non-zero off-diagonal entries can be arranged into a $k \times k$ submatrix by reordering rows and columns, then

$$J(\overline{f_{\mathbf{U}_{*1}, \dots, \mathbf{U}_{*(\delta+1)}}}) = 1 + O(k/p).$$

Hence, if $k = o(p)$ as $p \rightarrow \infty$, the quantity $J(\overline{f_{\mathbf{U}_{*1}, \dots, \mathbf{U}_{*(\delta+1)}}})$ converges to 1. If Σ is diagonal, then $J(\overline{f_{\mathbf{U}_{*1}, \dots, \mathbf{U}_{*(\delta+1)}}}) = 1$ exactly. In such cases, the quantity Λ_∞ in Corollary 2 does not depend on the unknown underlying distribution of the U-scores. As a result, the expected number of δ -hubs in $\mathcal{G}_\rho(\Psi)$ and the probability of discovery of at least one δ -hub do not depend on the underlying distribution. We will see in Sec. 4 that this result is useful in assigning statistical significance levels to vertices of the graph $\mathcal{G}_\rho(\Psi)$.

3.6 Phase Transitions and Critical Threshold

It can be seen from Theorem 2 and Corollary 2 that the number of δ -hub discoveries exhibits a phase transition in the high-dimensional regime where the number of variables p can be very large relative to the number of samples m . Specifically, assume that the population covariance matrix Σ is block-sparse as in Section 3.5. Then as the correlation threshold ρ is reduced, the number of δ -hub discoveries abruptly increases to the maximum, p . Conversely as ρ increases, the number of discoveries quickly approaches zero. Similarly, the family-wise error rate (i.e. the probability of discovering at least one δ -hub in a graph with no true hubs) exhibits a phase transition as a function of ρ . Figure 3 shows the family-wise error rate obtained via expression (32) for $\delta = 1$ and $p = 1000$, as a function of ρ and the number of samples m . It is seen that for a fixed value of m there is a sharp transition in the family-wise error rate as a function of ρ .

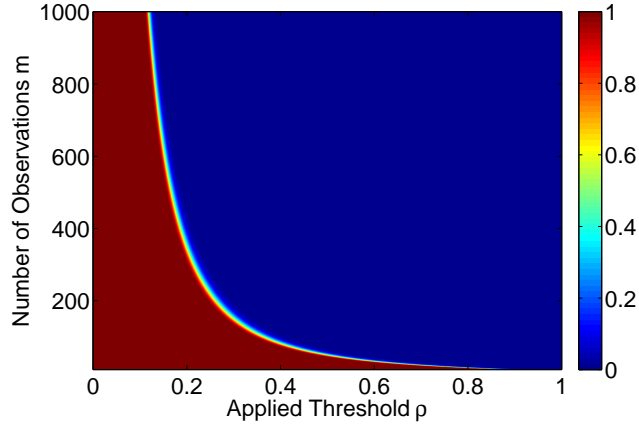


Fig. 3. Family-wise error rate as a function of correlation threshold ρ and number of samples m for $p = 1000, \delta = 1$. The phase transition phenomenon is clearly observable in the plot.

The phase transition phenomenon motivates the definition of a critical threshold $\rho_{c,\delta}$ as the threshold ρ satisfying the following slope condition:

$$\partial \mathbb{E}[N_{\delta,\rho}]/\partial \rho = -p.$$

Using (16) the solution of the above equation can be approximated via the expression below:

$$\rho_{c,\delta} = \sqrt{1 - (c_{m,\delta}(p-1))^{-2\delta/(\delta(2m-3)-2)}}, \quad (33)$$

where $c_{m,\delta} = b_{m-1} \delta J(\overline{f_{\mathbf{U}_{*1}, \dots, \mathbf{U}_{*(\delta+1)}}})$. The screening threshold ρ should be chosen greater than $\rho_{c,\delta}$ to prevent excessively large numbers of false positives. Note that the critical threshold $\rho_{c,\delta}$ also does not depend on the underlying distribution of the U-scores when the covariance matrix $\mathbf{\Sigma}$ is block-sparse.

Expression (33) is similar to the expression obtained in [9] for the critical threshold in real-valued correlation screening. However, in the complex-valued case the coefficient $c_{m,\delta}$ and the exponent of the term $c_{m,\delta}(p-1)$ are different from the real case. This generally results in smaller values of $\rho_{c,\delta}$ for fixed m and δ .

Figure 4 shows the value of $\rho_{c,\delta}$ obtained via (33) as a function of m for different values of δ and p . The critical threshold decreases as either the sample size m increases, the number of variables p decreases, or the vertex degree δ increases. Note that even for ten billion (10^{10}) dimensions (upper triplet of curves in the figure) only a relatively small number of samples are necessary for complex-valued correlation screening to be useful. For example, with $m = 200$ one can reliably discover connected vertices ($\delta = 1$ in the figure) having correlation greater than $\rho_{c,\delta} = 0.5$.

4 Application to Spectral Screening of Multivariate Gaussian Time Series

In this section, the complex-valued correlation hub screening method of Section 3 is applied to stationary multivariate Gaussian time series. Assume that the time series $X^{(1)}, \dots, X^{(p)}$ defined in Section 2 satisfy the conditions of Corollary 1. Assume also that a total of $N = n \times m$ time samples of $X^{(1)}, \dots, X^{(p)}$ are available. We divide the N samples into m parts of n consecutive samples and we take the n -point DFT of each part. Therefore, for each time series, at each frequency $f_i = (i-1)/n$, $1 \leq i \leq n$, m samples are available. This allows us to construct a (partial) correlation graph corresponding to each frequency. We denote the (partial) correlation graph corresponding to frequency f_i and correlation threshold ρ_i as $\mathcal{G}_{f_i, \rho_i}$. $\mathcal{G}_{f_i, \rho_i}$ has p vertices v_1, v_2, \dots, v_p corresponding to time series $X^{(1)}, X^{(2)}, \dots, X^{(p)}$, respectively. Vertices v_k and v_l are connected if the magnitude of the sample (partial) correlation between the DFTs of $X^{(k)}$ and $X^{(l)}$ at frequency f_i (i.e.

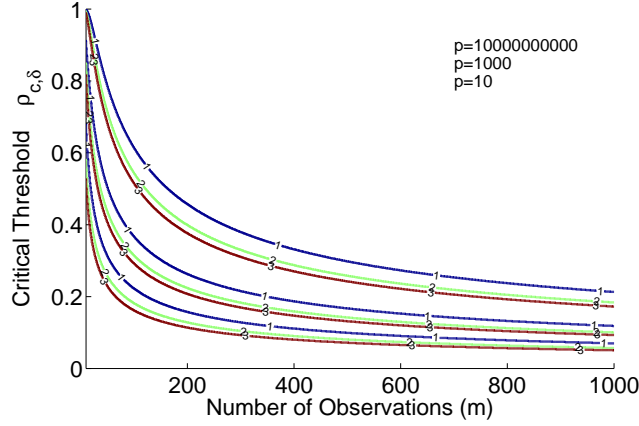


Fig. 4. The critical threshold $\rho_{c,\delta}$ as a function of the sample size m for $\delta = 1, 2, 3$ (curve labels) and $p = 10, 1000, 10^{10}$ (bottom to top triplets of curves). The figure shows that the critical threshold decreases as either m or δ increases. When the number of samples m is small the critical threshold is close to 1 in which case reliable hub discovery is impossible. However a relatively small increment in m is sufficient to reduce the critical threshold significantly. For example for $p = 10^{10}$, only $m = 200$ samples are enough to bring $\rho_{c,1}$ down to 0.5.

the sample (partial) correlation between $Y^{(k)}(i-1)$ and $Y^{(l)}(i-1)$ is at least ρ_i .

Consider a single frequency f_i and the null hypothesis, \mathcal{H}_0 , that the correlations among the time series $X^{(1)}, X^{(2)}, \dots, X^{(p)}$ at frequency f_i are block sparse in the sense of Section 3.5. As discussed in Sec. 3.5, under \mathcal{H}_0 the expected number of δ -hubs and the probability of discovery of at least one δ -hub in graph $\mathcal{G}_{f_i, \rho_i}$ are not functions of the unknown underlying distribution of the data. Therefore the results of Corollary 2 may be used to quantify the statistical significance of declaring vertices of $\mathcal{G}_{f_i, \rho_i}$ to be δ -hubs. The statistical significance is represented by the p-value, defined in general as the probability of having a test statistic at least as extreme as the value actually observed assuming that the null hypothesis \mathcal{H}_0 is true. In the case of correlation hub screening, the p-value $pv_\delta(j)$ assigned to vertex v_j for being a δ -hub is the maximal probability that v_j maintains degree δ given the observed sample correlations, assuming that the block-sparse hypothesis \mathcal{H}_0 is true. The detailed procedure for assigning p-values is similar to the procedure in [9] for real-valued correlation screening and is illustrated in Fig. 5. Equation (33) helps in choosing the initial threshold ρ^* .

Given Corollary 1, for $i \neq j$ the correlation graphs $\mathcal{G}_{f_i, \rho_i}$ and $\mathcal{G}_{f_j, \rho_j}$ and their associated inferences are approximately independent. Thus we can solve multiple inference problems by first performing correlation hub screening on

- Initialization:
 1. Choose a degree threshold $\delta \geq 1$.
 2. Choose an initial threshold $\rho^* > \rho_{c,\delta}$.
 3. Calculate the degree d_j of each vertex of graph $\mathcal{G}_{\rho^*}(\Psi)$.
 4. Select a value of $\delta \in \{1, \dots, \max_{1 \leq j \leq p} d_j\}$.
- For each $j = 1, \dots, p$ find $\rho_j(\delta)$ as the δ th greatest element of the j th row of the sample (partial) correlation matrix.
- Approximate the p-value corresponding to vertex v_j as $pv_\delta(j) \approx 1 - \exp(-\mathbb{E}[N_{\delta,\rho_j(\delta)}]/\varphi(\delta))$, where $\mathbb{E}[N_{\delta,\rho_j(\delta)}]$ is approximated by the limiting expression (31) using $J(\mathbf{f}_{\mathbf{U}_{*1}, \dots, \mathbf{U}_{*(\delta+1)}}) = 1$.
- Screen variables by thresholding the p-values $pv_\delta(j)$ at desired significance level.

Fig. 5. Procedure for assigning p-values to the vertices of $\mathcal{G}_{\rho^*}(\Psi)$.

each graph as discussed above and then aggregating the inferences at each frequency in a straightforward manner. Examples of aggregation procedures are described below.

4.1 Disjunctive Hubs

One task that can be easily performed is finding the p-value for a given time series to be a hub in at least one of the graphs $\mathcal{G}_{f_1, \rho_1}, \dots, \mathcal{G}_{f_n, \rho_n}$. More specifically, for each $j = 1, \dots, p$ denote the p-values for vertex v_j being a δ -hub in $\mathcal{G}_{f_1, \rho_1}, \dots, \mathcal{G}_{f_n, \rho_n}$ by $pv_{f_1, \rho_1, \delta}(j), \dots, pv_{f_n, \rho_n, \delta}(j)$ respectively. These p-values are obtained using the method of Fig. 5. Then $pv_\delta(j)$, the p-value for the vertex v_j being a δ -hub in at least one of the frequency graphs $\mathcal{G}_{f_1, \rho_1}, \dots, \mathcal{G}_{f_n, \rho_n}$ can be approximated as:

$$\mathbb{P}(\exists i : d_{j, f_i} \geq \delta \mid \mathcal{H}_0) \approx \hat{p}v_\delta(j) = 1 - \prod_{i=1}^n (1 - pv_{f_i, \rho_i, \delta}(j)),$$

in which d_{j, f_i} is the degree of v_j in the graph $\mathcal{G}_{f_i, \rho_i}$.

4.2 Conjunctive Hubs

Another property of interest is the existence of a hub at all frequencies for a particular time series. In this case we have:

$$\mathbb{P}(\forall i : d_{j, f_i} \geq \delta \mid \mathcal{H}_0) \approx \check{p}v_\delta(j) = \prod_{i=1}^n pv_{f_i, \rho_i, \delta}(j).$$

4.3 General Persistent Hubs

The general case is the event that at least K frequencies have hubs of degree at least δ at vertex v_j . For this general case we have:

$$\mathbb{P}(\exists i_1, \dots, i_K : d_{j, f_{i_1}} \geq \delta, \dots, d_{j, f_{i_K}} \geq \delta \mid \mathcal{H}_0) = \sum_{k'=K}^n \sum_{\substack{i_1 < \dots < i_{k'}, i_{k'+1} < \dots < i_n \\ \{i_1, \dots, i_n\} = \{1, \dots, n\}}} \prod_{l=1}^{k'} p_{v_{f_{i_l}}, \rho_{i_l}, \delta}(j) \prod_{l'=k'+1}^n \left(1 - p_{v_{f_{i_{l'}}, \rho_{i_{l'}}, \delta}(j)}\right).$$

5 Experimental Results

5.1 Phase Transition Phenomenon and Mean Number of Hubs

We first performed numerical simulations to confirm Theorem 2 and Corollary 2 for complex-valued correlation screening. Samples were generated from p uncorrelated complex Gaussian random variables. Figure 6 shows the number of discovered 1-hubs for $p = 1000$ and several sample sizes m . The plots from left to right correspond to $m = 2000, 1000, 500, 100, 50, 20, 10, 6$ and 4, respectively. The phase transition phenomenon is clearly observed in the plot. Table 1 shows the predicted value obtained from formula (33) for the critical threshold. As can be seen in Fig. 6, the empirical phase transition thresholds approximately match the predicted values of Table 1. Moreover, to confirm the accuracy of equation (31) in Corollary 2, we list the number of hubs for $m = 100$ in Table 2. The left column shows the empirical average number of hubs of degree at least $\delta = 1, 2, 3, 4$ in a network of i.i.d. complex Gaussian random variables. The numbers in this column are obtained by averaging 1000 independent experiments. The right column shows the predicted value of $\mathbb{E}[N_{\delta, \rho}]$ obtained via formula (31) with $J(\overline{f_{\mathbf{U}_{*1}, \dots, \mathbf{U}_{*(\delta+1)}}}) = 1$ for the i.i.d. case. As we see the empirical and predicted values are close to each other.

m	2000	1000	500	100	50	20	10	6	4
$\rho_{c, \delta}$	0.05	0.07	0.10	0.24	0.35	0.56	0.78	0.94	0.99

Table 1. The value of critical threshold $\rho_{c, \delta}$ obtained from formula (33) for $p = 1000$ complex variables and $\delta = 1$. The predicted $\rho_{c, \delta}$ approximates the phase transition thresholds in Fig. 6.

5.2 Asymptotic Independence of Spectral Components for AR(1) Model

To illustrate the asymptotic independence property and convergence rate of Theorem 1, we considered the simple case of an AR(1) process,

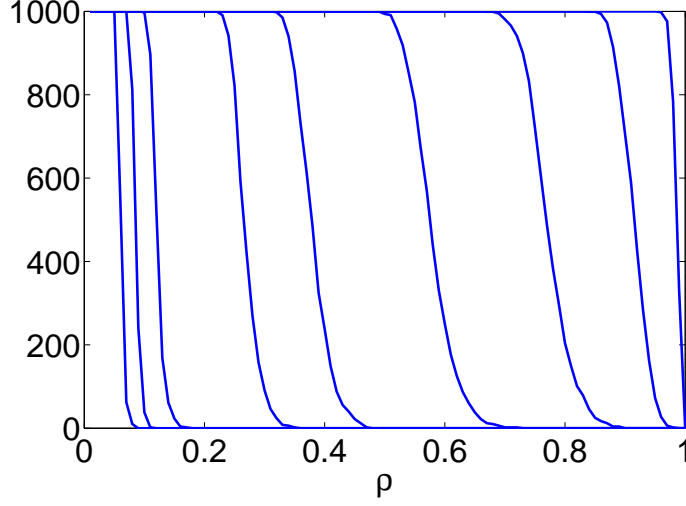


Fig. 6. Phase transition phenomenon: the number of 1-hubs in the sample correlation graph corresponding to uncorrelated complex Gaussian variables as a function of correlation threshold ρ . Here, $p = 1000$ and the plots from left to right correspond to $m = 2000, 1000, 500, 100, 50, 20, 10, 6$ and 4 , respectively.

degree threshold	empirical ($\mathbb{E}[N_{\delta,\rho}]$)	predicted ($\mathbb{E}[N_{\delta,\rho}]$)
$d_i \geq \delta = 1$	284	335
$d_i \geq \delta = 2$	45	56
$d_i \geq \delta = 3$	5	6
$d_i \geq \delta = 4$	0	0

Table 2. Empirical average number of discovered hubs vs. predicted average number of discovered hubs in an uncorrelated complex Gaussian network. Here $p = 1000$, $m = 100$, $\rho = 0.28$. The empirical values are obtained by performing 1000 independent experiments.

$$X(k) = \varphi_1 X(k-1) + \varepsilon(k), \quad k \geq 1, \quad (34)$$

in which $X(0) = 0$, $\varphi_1 = 0.9$ and $\varepsilon(\cdot)$ is a stationary Gaussian process with no temporal correlation and standard deviation 1. We performed Monte-Carlo simulations to compute the correlation between spectral components at different frequencies for window sizes $n = 10, 20, \dots, 250$. More specifically, we set $k = 1$ and $l = 2$ and empirically estimated $|\text{cor}(Y(k), Y(l))|$ using 50000 Monte-Carlo trials for each value of window size n . Figure 7 shows the result of this experiment. It is observable that the magnitude of $\text{cor}(Y(k), Y(l))$ is bounded above by the function $10/n$. This observation is consistent with Theorem 1.

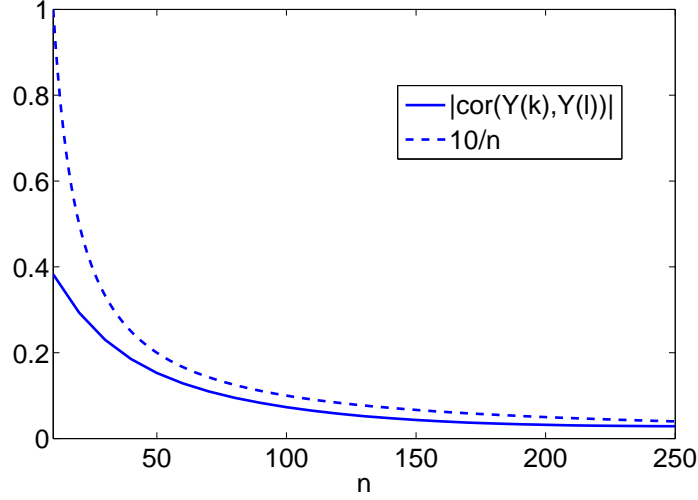


Fig. 7. Correlation coefficient $|\text{cor}(Y(1), Y(2))|$ as a function of window size n , empirically estimated using 50000 Monte-Carlo trials. Here $Y(\cdot)$ is the DFT of the AR(1) process (34). The magnitude of the correlation for $n = 10, 20, \dots, 250$ is bounded above by the function $10/n$. This observation is consistent with the convergence rate in Theorem 1.

5.3 Spectral Correlation Screening of a Band-Pass Multivariate Time Series

Next we analyzed the performance of the proposed complex-valued correlation screening framework on a synthetic data set for which the expected results are known.

We synthesized a multivariate stationary Gaussian time series using the following procedure. Here we set $p = 1000$, $N = 12000$ and $m = n = 100$. The discrepancy between N and the product mn is explained below. Let $X(k)$, $0 \leq k \leq N - 1$ be a sequence of i.i.d. zero-mean Gaussian random variables (i.e. white Gaussian noise) with standard deviation of 1. The p time series $X^{(1)}(k), \dots, X^{(p)}(k)$, $0 \leq k \leq N - 1$ are obtained from $X(k)$ by band-pass filtering and adding independent white Gaussian noise. Specifically,

$$X^{(i)}(k) = h_i(k) \star X(k) + N_i(k), \quad 1 \leq i \leq p, 0 \leq k \leq N - 1,$$

in which \star represents the convolution operator, $h_i(\cdot)$ is the impulse response of the i th band-pass filter and $N_i(\cdot)$ is an independent white Gaussian noise series whose standard deviation is 0.1. Since stable filtering of a stationary series results in another stationary series, the obtained series $X^{(1)}(k), \dots, X^{(p)}(k)$ are stationary and Gaussian. For $i = 10l$, $1 \leq l \leq 50$, $h_i(k)$ is the impulse response of a band-pass filter with pass band $f \in [(4l - 1)/400, 4l/400]$. We

approximate the ideal band-pass filters with finite impulse response (FIR) Chebyshev filters [16]. Also for $i = 500 + 10l, 1 \leq l \leq 50$ we set $h_i(k) = h_{i-500}(k)$. For all of the other values of i (i.e. $i \neq 10l$) we set $h_i(k) = 0, 0 \leq k \leq N - 1$.

Figure 8 shows the signal part of the time series (i.e. $h_i(k) \star X(k)$) for $i = 100, 200, 300, 400$. It is seen that the first 2000 samples of the signals reflect the transient response of the filters. These 2000 samples are not included for the purpose of correlation screening. Hence the actual number of time samples considered is $mn = 10000$. Figure 9 shows the magnitude of the DFTs of the signals, $Y^{(i)}(k)$, for $i = 50, 100, \dots, 500$. The band-pass structure of the signals is clearly observable in the figure.

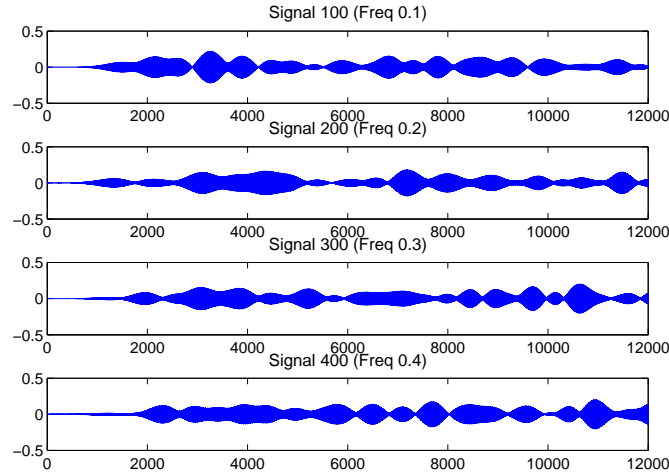


Fig. 8. Signal part of the band-pass time series $X^{(i)}(k)$ (i.e. $h_i(k) \star X(k)$) for $i = 100, 200, 300, 400$.

We first constructed a correlation matrix for the time series $X^{(1)}(k), \dots, X^{(p)}(k)$ from their simultaneous time samples. Figure 10 illustrates the structure of the thresholded sample correlation matrix and the corresponding correlation graph. Note that this is a real-valued correlation screening problem in the time domain. The correlation threshold used here is $\rho = 0.2$ which is well above the critical threshold $\rho_{c,1} = 0.028$ obtained via formula (10) in [9] for $p = 1000$ and $N = 10000$.

To examine the spectral structure of the correlations in Fig. 10, we then performed complex-valued correlation screening on the spectra of the time series $X^{(1)}(k), \dots, X^{(p)}(k)$. Figure 11 shows the constructed correlation graphs $\mathcal{G}_{f,\rho}$ for $f = [0.1, 0.2, 0.3, 0.4]$ and correlation threshold $\rho = 0.9$, which corre-

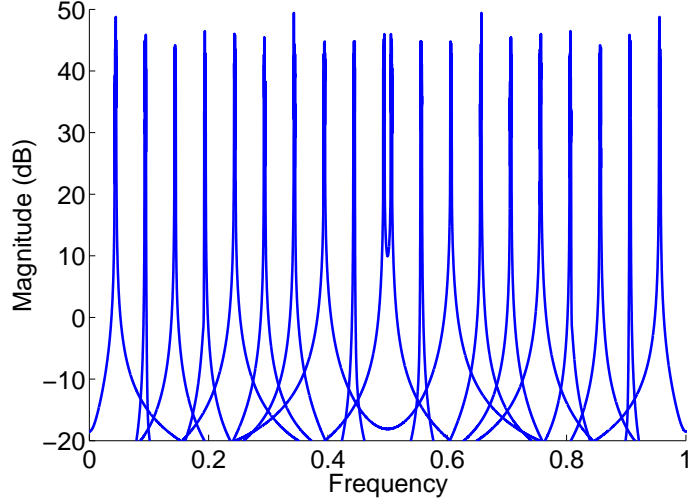


Fig. 9. DFT magnitude of the band-pass signals $h_i(k) \star X(k)$ (i.e. $20 \log_{10}(|Y^{(i)}(\cdot)|)$) as a function of frequency for $i = 50, 100, \dots, 500$.

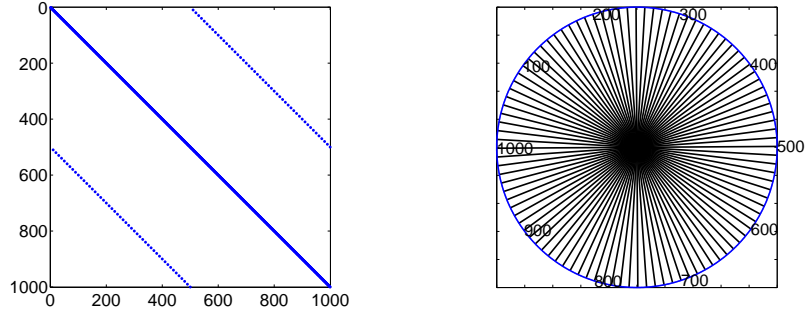


Fig. 10. (Left) The structure of the thresholded sample correlation matrix in the time domain. (Right) The correlation graph corresponding to the thresholded sample correlation matrix in the time domain.

sponds to a $\delta = 1$ false positive rate $\mathbb{P}(N_{\delta, \rho} > 0) \approx 10^{-65}$ (using $\delta = 1$ in the asymptotic relation (32) with $\Lambda_\infty = e_{m, \delta}^\delta / \delta!$ as specified by (31)). Note that the value of the correlation threshold is set to be higher than the critical threshold $\rho_c = 0.24$. It can be observed that performing complex-valued spectral correlation screening at each frequency correctly discovers the correlations between the time series which are active around that frequency. As an example, for $f = 0.2$ the discovered hubs (for $\delta = 1$) are the time series $X^{(i)}(k)$ for $i \in \{200, 700\}$. These time series are the ones that are active at

frequency $f = 0.2$. Under the null hypothesis of diagonal covariance matrices, the p-values for the discovered hubs are of order 10^{-65} or smaller. These results show that complex-valued spectral correlation screening is able to resolve the sources of correlation between time series in the spectral domain.

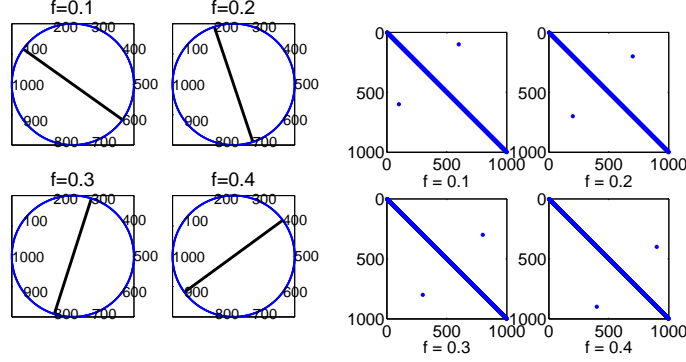


Fig. 11. Spectral correlation graphs $\mathcal{G}_{f,\rho}$ for $f = [0.1, 0.2, 0.3, 0.4]$ and correlation threshold $\rho = 0.9$, which corresponds to a false positive probability of 10^{-65} . The data used here is a set of synthetic time series obtained by band-pass filtering of a Gaussian white noise series with the band-pass filters shown in Fig. 9. As can be seen, complex correlation screening is able to extract the correlations at specific frequencies. This is not directly feasible in the time domain analysis.

6 Conclusion

This chapter presented a spectral method for correlation analysis of stationary multivariate Gaussian time series with a focus on identifying correlation hubs. The asymptotic independence of spectral components at different frequencies allows the problem to be decomposed into independent problems at each frequency, thus improving computational and statistical efficiency for high-dimensional time series. The method of complex-valued correlation screening is then applied to detect hub variables at each frequency. Using a characterization of the number of hubs discovered by the method, thresholds for hub screening can be selected to avoid an excessive number of false positives or negatives, and the statistical significance of hub discoveries can be quantified. The theory specifically considers the high-dimensional case where the number of samples at each frequency can be significantly smaller than the number of time series. Experimental results validated the theory and illustrated the applicability of complex-valued correlation screening to the spectral domain.

7 Acknowledgment

This work was partially supported by AFOSR grant FA9550-13-1-0043.

References

1. Vuran, M.C., Akan, Ö.B., Akyildiz, I.F.: Spatio-temporal correlation: theory and applications for wireless sensor networks. *Computer Networks* **45**(3), 245–259 (2004)
2. Paffenroth, R., du Toit, P., Nong, R., Scharf, L., Jayasumana, A.P., Bandara, V.: Space-time signal processing for distributed pattern detection in sensor networks. *Selected Topics in Signal Processing, IEEE Journal of* **7**(1), 38–49 (2013)
3. Friston, K.J., Ashburner, J.T., Kiebel, S.J., Nichols, T.E., Penny, W.D.: *Statistical Parametric Mapping: The Analysis of Functional Brain Images: The Analysis of Functional Brain Images*. Academic Press (2011)
4. Zhang, P., Huang, Y., Shekhar, S., Kumar, V.: Correlation analysis of spatial time series datasets: A filter-and-refine approach. In: *Advances in Knowledge Discovery and Data Mining*, pp. 532–544. Springer (2003)
5. Tsay, R.S.: *Analysis of financial time series*, vol. 543. Wiley. com (2005)
6. Stanley, M., Gervais-Ducouret, S., Adams, J.: Intelligent sensor hub benefits for wireless sensor networks. In: *Sensors Applications Symposium (SAS)*, 2012 IEEE, pp. 1–6. IEEE (2012)
7. Li, Y., Thai, M.T., Wu, W.: *Wireless sensor networks and applications*. Springer (2008)
8. Bullmore, E., Sporns, O.: Complex brain networks: graph theoretical analysis of structural and functional systems. *Nature Reviews Neuroscience* **10**(3), 186–198 (2009)
9. Hero, A., Rajaratnam, B.: Hub discovery in partial correlation graphs. *Information Theory, IEEE Transactions on* **58**(9), 6064–6078 (2012)
10. Chen, X., Xu, M., Wu, W.B., et al.: Covariance and precision matrix estimation for high-dimensional time series. *The Annals of Statistics* **41**(6), 2994–3021 (2013)
11. Hero, A., Rajaratnam, B.: Large-scale correlation screening. *Journal of the American Statistical Association* **106**(496), 1540–1552 (2011)
12. Firouzi, H., Rajaratnam, B., Hero, A.: Predictive correlation screening: Application to two-stage predictor design in high dimension. In: *Proceedings of the Sixteenth International Conference on Artificial Intelligence and Statistics (AISTATS)* (2013)
13. Durrett, R.: *Probability: theory and examples*, vol. 3. Cambridge university press (2010)
14. Grenander, U., Szegő, G.: *Toeplitz forms and their applications*. Univ of California Press (1958)
15. Gray, R.M.: Toeplitz and circulant matrices: A review. *Foundations and Trends in Communications and Information Theory* **2**(3), 155–239 (2006). DOI 10.1561/01000000006. URL <http://dx.doi.org/10.1561/01000000006>
16. Oppenheim, A.V., Schaffer, R.W., Buck, J.R., et al.: *Discrete-time signal processing*, vol. 2. Prentice-hall Englewood Cliffs (1989)

17. Conway, J.B.: A course in functional analysis, vol. 96. Springer (1990)
18. Hamilton, J.D.: Time series analysis, vol. 2. Princeton university press Princeton (1994)
19. Micheas, A.C., Dey, D.K., Mardia, K.V.: Complex elliptical distributions with application to shape analysis. *Journal of statistical planning and inference* **136**(9), 2961–2982 (2006)
20. Simon, M.K.: Probability distributions involving Gaussian random variables: A handbook for engineers and scientists. Springer (2007)
21. Arratia, R., Goldstein, L., Gordon, L.: Poisson approximation and the Chen-Stein method. *Statistical Science* **5**(4), 403–424 (1990)